RESILIENT INFRASTRUCTURE
June 1–4, 2016
RESILIENT INFRASTRUCTURE LONDON 2016

THE EFFECT OF TEMPERATURE ON THE LATERAL RESPONSE OF UNBONDED FIBER-REINFORCED ELASTOMERIC ISOLATORS

Alexander N. Sciascetti
M.A.Sc. Student, McMaster University, Canada.

Yasser M. Al-Anany
Ph.D. Candidate, McMaster University, Canada.

Michael J. Tait
Professor, JNE Consulting Chair in Design, Construction, and Management in Infrastructure Renewal, McMaster University, Canada

ABSTRACT

Base isolation is a method that can be employed to significantly reduce the demands on a structure during a seismic event. This method has shown considerable success in reducing the adverse effects of earthquakes, including damage and loss of life. The main concept of base isolation is to reduce the seismic demand on a structure by placing isolators beneath the superstructure at points where load is transferred to the foundation. One of the most commonly used types of isolator is the elastomeric isolator. These isolators are traditionally comprised of layers of elastomer and steel. More recently, research has been completed on the use of fibers as a replacement to the steel reinforcement layers, in order to reduce weight and potentially reduce costs. Fiber reinforced elastomeric isolators (FREI) can be placed (unbonded) between the superstructure and its foundation. This research investigates the behaviour of unbonded fiber-reinforced elastomeric isolators (U-FREI) under lateral deformations expected during seismic events. The objective of this study is to investigate the lateral behaviour of FREI under a range of temperatures, representative of those expected in various regions throughout Canada. Results from preliminary experimental tests show that the influence of temperature on the lateral response of U-FREI is negligible under the range of temperatures considered.

Keywords: bridge structures; base isolation; fiber-reinforced; temperature; lateral response

1. INTRODUCTION

Fiber reinforced elastomeric isolators (FREI) have been investigated as a potentially lighter and less expensive alternative to traditional steel reinforced elastomeric isolators. Several studies have shown that by using a fiber material (such as carbon fiber) with an elastic modulus on the same order as steel, the vertical stiffness requirement of the bearing can be satisfied (Kelly 1999; Al-Anany et al. 2016a). The individual fibers are twisted into larger strands, which are woven together to form the thin layer of material that is used as the reinforcement. When tension is applied along the axis of the fiber strands, they straighten and allow the fabric to stretch. Accordingly, if fiber is used for reinforcement instead of steel, the flexibility of the isolator in extension is expected to increase while its flexural rigidity would decrease. It has been shown that a reduction in the flexural rigidity has a limited effect on the horizontal stiffness of a bonded FREI, as the stiffness decrease is only on the order of 10% when compared to laminated steel bearings (Kelly 1999).

The application of unbonded FREI (U-FREI) also presents desirable properties that are exhibited at larger shear strains. It was shown by Toopchi-Nezhad et al. (2007) that with the appropriate aspect ratio (width to total height ratio), a rollover mechanism develops, which results in a decrease in the effective lateral stiffness as the lateral displacement increases. The initial decrease in stiffness corresponds to a change in boundary conditions as the bearing begins to rollover. The rollover mechanism is stable when positive lateral tangent stiffness is observed

throughout the hysteresis loop (Toopchi-Nezhad et al. 2008a). Further research by Van Engelen et al. (2014) found that as the aspect ratio is decreased, the bearing becomes more susceptible to experiencing unstable rollover behaviour. In addition, it was determined that aspect ratios over 2.5 allow the rollover mechanism to be stable (Van Engelen et al. 2014). Under very large lateral displacement amplitudes a hardening behaviour occurs, which is associated with the bearing rolling over onto its vertical faces. At this point the vertical faces become horizontal and are in complete contact with the upper and lower loading platens. This contact is expected to limit the maximum lateral displacement of the bearing and prevents a negative tangent stiffness from occurring at large displacements (de Raaf et al. 2011).

Recently, unbonded FREI bearings were evaluated analytically (Al-Anany and Tait 2015) and experimentally (Al-Anany and Tait 2016b) to determine their behaviour under the vertical and rotational loading that is typical of bridge bearings. It was shown that unbonded FREI bearings meet criteria in CSA-S6 and AASHTO-LRFD by investigating the bearing behaviour under vertical stresses up to 10 MPa and angles of rotation up to 0.05 radians. With respect to this application of FREI bearings in bridges, the bearings must also withstand the same negative temperatures that the bridge itself experiences. Roeder et al. (1989) studied the low temperature behaviour of elastomeric isolators and concluded that temperature has a large effect on the stiffness of the bearing. Results from this study also confirmed that there are two main mechanisms that cause stiffening: instantaneous thermal stiffening and low temperature crystallization. Thermal stiffening is independent of time and is a function of temperature only. As the temperature is decreased, the rubber begins to stiffen immediately. Once below the second order transition temperature of the material, the increase in stiffness can be more than 50 times its room temperature value (Roeder et al. 1989). The second order transition temperature has been suggested to be approximately -60 °C for natural rubber and -50 °C for neoprene (Roeder et al. 1990). The second mechanism, low temperature crystallization, occurs after an initial delay from the time that the temperature was decreased. The bearing then begins to increase in stiffness before it ultimately plateaus. As the temperature is decreased, the delay becomes longer, the rate of increase in stiffness grows and produces a higher plateau (Roeder et al. 1989). Murray and Detenber (1961) and Roeder et al. (1990) both reported that low temperature crystallization has less of an effect on natural rubber than neoprene compounds. As a result, it was suggested that natural rubber bearings are more suitable for low temperatures. The rate of stiffness increase was slower and the plateau was much lower for the natural rubber. It was found that the natural rubber in some instances had not reached its plateau stiffness even after 21 days at the conditioning temperature (Roeder et al. 1990).

The results from Roeder are reflected in the AASHTO Standard Specification for Plain and Laminated Elastomeric Bridge Bearings (2006). The standard splits bearings into five grades based on service location, where each grade is to be tested for shear modulus at low temperatures for extended periods of time. For example, a Grade 2 bearing must be conditioned for 7 days at -18 ± 2 °C, while a Grade 5 bearing must be conditioned for 28 days at -37 ± 2 °C (AASHTO 2006). This insures that the peak stiffness of the bearing is known once it plateaus. Roeder et al. (1989) recommended that the conditioned bearing's stiffness must be less than four times the stiffness at room temperature. This was adopted by AASHTO as the pass criteria for conditioned bearing stiffness testing. In the CSA Canadian Highway Bridge Design Code (2014), it is required of bearings to be conditioned for 14 days at a temperature equal to the minimum mean daily temperature for the service location of the bearing. The CSA code also specifies the conditioning temperature criteria for a 2% probability of exceedance. The temperature is taken as the average of two values, 15 °C and the minimum service temperature (CSA-S6 2014).

These studies confirm that a large increase in stiffness is of concern to engineers designing bridge bearings in cold climates. In Canada, bridge bearings can be subject to a large range of temperatures and the stiffness of the isolators must be limited in order to reduce the shear forces that can be transferred to the bridge during earthquakes. The objective of this paper is to evaluate the effect of low temperatures on the lateral response of unbonded, natural rubber FREI. The considered bearings are designed with the ability to exhibit stable rollover.

2. TEST SPECIMENS

The FREI specimens were cut from a larger pad that was constructed in the Applied Dynamics Laboratory (ADL) at McMaster University. This pad was formed using natural rubber with a shear modulus of approximately 0.85 MPa and bi-directional carbon fiber cloth with 0 and 90 degree orientations. Seven layers of rubber were used, with the upper and lower layers half the thickness of the internal layers. A hot-vulcanization bonding agent was used to fuse

the layers of rubber and fiber reinforcement together. The total height of the rubber (t_r) in the final pad was 17 mm. The pad was then cut into four ¼-scale FREI using a band saw, with each bearing having an aspect ratio of 3.
The first bearing was kept at room temperature, 20 ± 5 °C in order to serve as a base line. The temperature of the second bearing was held at 0 °C by placing it in a freezer where it was conditioned for seven days. The third specimen was held at a temperature that was very similar to that required for a Grade 2 AASHTO bearing. It was placed in a freezer at -20 °C where it was also conditioned for seven days. In this initial pilot study, a shorter conditioning time was used in order to lower the wait time of the initial study. Further studies to determine how the FREI bearings behave under more extreme conditions are currently being carried out.

3. TEST SETUP AND PROCEDURE

The FREI were tested using a setup that is capable of applying vertical and lateral displacements to the specimen. The setup consists of a reaction frame, a loading beam and a pedestal. The pedestal consists of a large column section attached at the base, with a lower platen, two 3-axis load cells, and an upper platen fixed on top. The specimen is placed on the upper platen and is loaded vertically using two vertical actuators attached to opposite sides of the loading beam. The actuators use the 3-axis load cells to ensure that the target vertical load is maintained. A lateral actuator, which is attached to the end of the loading beam, is used to apply lateral displacements. A string potentiometer records these displacements at the center of the loading beam with reference to the stationary reaction frame. Between the upper platen and the loading beam are two removable steel plates that facilitate the addition of surfaces with varied coefficients of friction. In this study, smaller steel plates, roughened to have a coefficient of friction similar to that of concrete, were installed onto the removable steel plates. The unbonded FREI test specimens were placed between the roughened plates for testing. For the low temperature tests, the removable plates with the installed roughened surface were placed in the same freezer unit as the specimen. This ensured that the bearings did not experience a sudden increase in temperature when placed in the test setup, as it was expected that a thin layer of water would have formed between the test specimen and the roughened plates that could induce slip during testing if they had not been placed in the freezer (Pinarbasi et al. 2007).

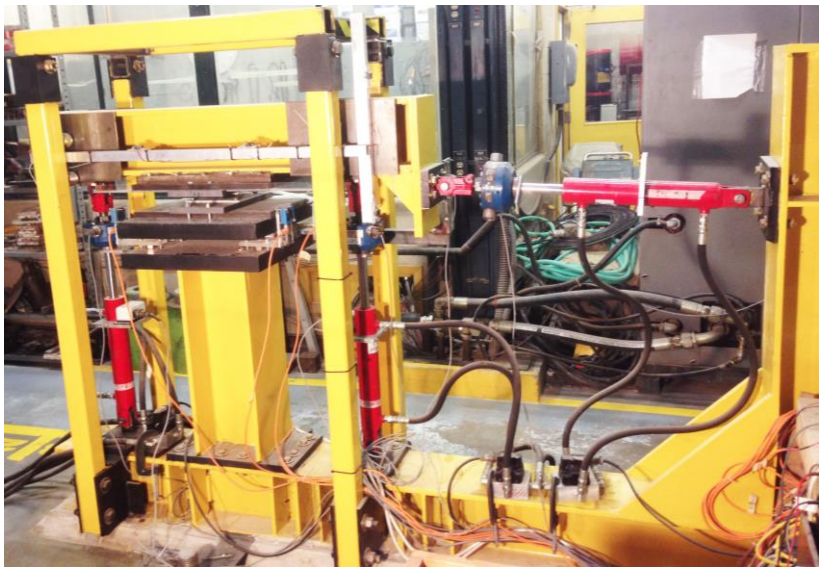

Figure 1: Photograph of test setup.

Once the conditioning period was complete, the steel plates were first removed from the freezer and rapidly installed into the test setup. The FREI specimen was then removed from the freezer and placed in the setup, where the test commenced. The total time to complete the test was less than 60 seconds. Each specimen was subject to a constant vertical pressure of 7 MPa, applied using a ramp function as shown in Figure 2. The lateral cyclic displacement was applied once the vertical pressure was achieved and consisted of three, fully reversed, sinusoidal cycles at each horizontal amplitude equalling a percentage of the total thickness of rubber layers, t_r. These lateral amplitudes in sequence were 25%, 50%, 75%, 100%, 150%, 200% of t_r as given in Figure 2. After the three cycles at 200% t_r were completed, the specimen was vertically unloaded.

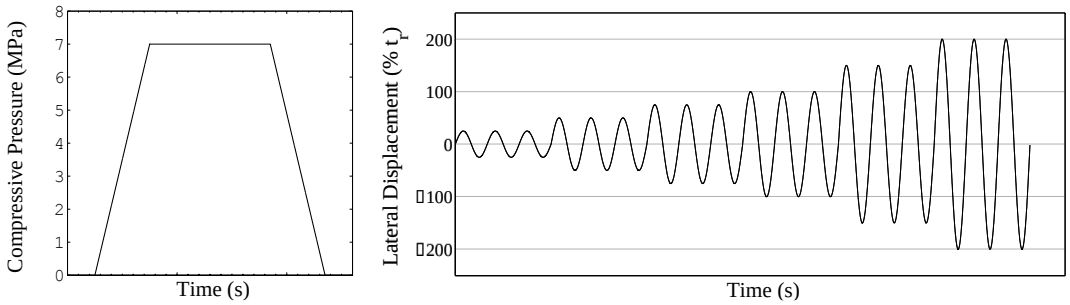

Figure 2: Vertical loading time history (left). Lateral displacmenet time history (right).

From each cycle, the effective horizontal stiffness of the specimen can be found. It is calculated as the slope of the line that connects the maximum lateral load and corresponding displacement with the minimum lateral load and displacement (ASCE 2010).

$$[1]\ K_{h.eff} = (F_{max}\text{-}F_{min})/(\Delta_{max}\text{-}\Delta_{min})$$

The variables of F_{max}, F_{min}, Δ_{max}, and Δ_{min} are the maximum and minimum values of lateral load and displacement. The effective horizontal stiffness, as well as the equivalent viscous damping ratio, are calculated for each full cycle of displacement. The equation used to calculate the damping ratio is given below (Chopra 2012):

$$[2]\ \zeta = \frac{E_D}{2\pi K_{h,eff}\Delta_{avg}^2} \quad \text{where} \quad \Delta_{avg} = \frac{\Delta_{max} + |\Delta_{min}|}{2}$$

The variable E_D is the area enclosed by the hysteresis loop for a particular cycle. It represents the energy dissipated in that individual cycle and is equated with that of an equivalent viscously damped system.

4. LATERAL RESPONSE

4.1 Specimen Hysteresis Analysis

The first FREI was tested at room temperature and subject to the sequence of lateral displacement amplitudes as described above. The test was videotaped in order to review the test and confirm that slip did not occur with the specimen. It can be seen in Figure 3 that the FREI exhibited acceptable behaviour and remained stable over the entirety of the test.

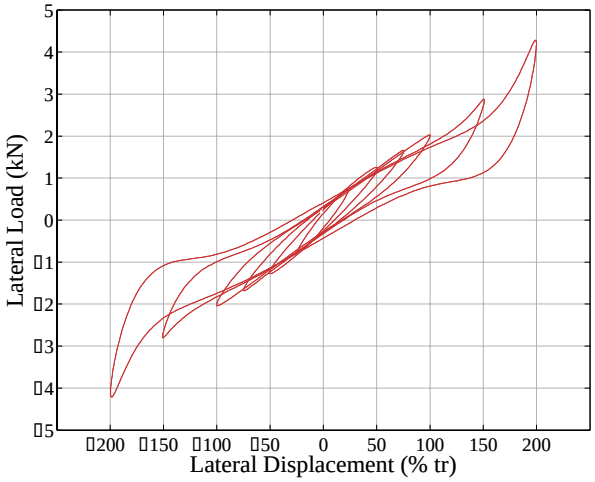

Figure 3: 20 °C hysteresis loops corresponding to the final cycle at each lateral displacement amplitude.

As the displacement amplitude was increased from 25% t_r to 100% t_r, the effective stiffness of each cycle decreased. At even larger lateral displacements, the vertical faces of the FREI were close to becoming completely horizontal, but did not make contact with the loading platens. Finally, at 200% t_r, it was observed that full rollover occurred. The slope of the curve begins to decrease at around 50% t_r, but then starts to increase again around 125% t_r. This slope change becomes more prominent between 150% and 200% t_r where it can be seen to continue to increase and pick up lateral load. The maximum absolute value of lateral load from the final 200% t_r cycle was 4284 N.

As previous mentioned the second FREI test specimen was conditioned for 7 days at 0 ± 3 °C. Based on the elastomer used, the FREI was not expected to exhibit behaviour that differed greatly from the first specimen at room temperature. At 0 °C, the rubber is not at a low enough temperature to have a large rate of crystallization. As a result, any increase in stiffness was expected to be minimal and primarily due to instantaneous thermal stiffening. A video recording of the test was reviewed to confirm that no slippage occurred.

It can be seen from Figure 4a that the peak force achieved was 4724 N. This value is approximately 500 N larger than the maximum value for the FREI tested at room temperature, which indicates an increase in the effective stiffness. In addition, the video recording showed that the bearing was able to exhibit a full, stable rollover at 200% t_r, despite the increase in stiffness. In general, it can also be seen in Figure 4a that the hysteresis loops for the 0 °C specimen contain a slightly larger area than those for the original specimen. This implies that the bearing was able dissipated more energy and should have a higher equivalent viscous damping ratio.

The final FREI test specimen was conditioned at -20 ± 3 °C for 7 days. This bearing was expected to be stiffer than the previous two specimens, as instantaneous thermal stiffening would have a greater effect at this temperature. In addition, it was expected to gain more stiffness due to crystallization, since the rate of stiffness increase is greater at lower temperatures. The hysteresis loops for this test specimen, which are shown in Figure 4b, indicate acceptable behaviour as positive tangential stiffness is maintained. A peak force of 4723 N was required to displace the bearing to the 200% t_r cycle and it can be seen that this specimen was not pushed fully to the end of each cycle. The deformation was 2% t_r short of being displaced to the full amplitude of 200% t_r, but had already reached the same lateral load as the 0 °C bearing, indicating that it was more stiff. Lastly, it can be seen that the hysteresis loops of this bearing contain more area, indicating that this bearing was able to dissipate more energy and as a result should have a larger damping ratio.

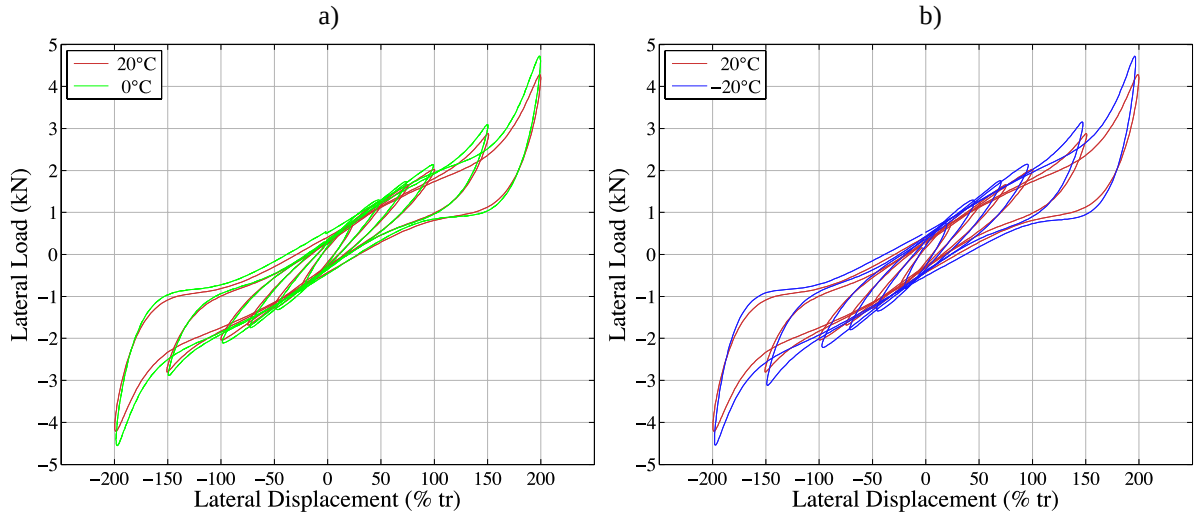

Figure 4: 0 °C (a) and -20 °C (b) hysteresis loops overlaid 20 °C hysteresis loops corresponding to the final cycle at each lateral displacement amplitude.

4.2 Effective Stiffness Comparisons

Additional information on the difference between the three conditioning temperatures can be obtained through the calculated lateral stiffness and damping. These values are given for each cycle in Table 1. The effective stiffness of

each specimen for the third cycle at each lateral displacement amplitude are presented in Figure 5a. This figure provides a graphical representation of the change in horizontal stiffness as the FREI are subjected to increasing displacements.

Table 1: Effective stiffness and damping at different temperatures.

Displacement Amplitude	Cycle	20 ºC		0 ºC		-20 ºC	
		Stiffness (N/mm)	Damping (%)	Stiffness (N/mm)	Damping (%)	Stiffness (N/mm)	Damping (%)
25% t_r [a]	1	194.8	11.4	217.7	13.2	241.8	15.1
	2	189.6	11.9	211.8	13.7	235.1	16.1
	3	186.0	11.5	208.1	13.4	229.9	15.6
50% t_r	1	159.2	10.0	174.3	11.1	187.7	12.9
	2	148.8	9.9	161.2	10.9	172.4	12.8
	3	146.5	9.7	158.7	10.7	169.6	12.6
75% t_r	1	140.2	9.3	151.2	10.1	160.9	11.7
	2	133.3	8.7	142.7	9.6	150.5	11.3
	3	130.7	8.7	139.7	9.5	147.2	11.3
100% t_r	1	130.8	8.5	139.8	9.2	148.4	10.5
	2	122.0	8.3	129.4	9.0	136.4	10.4
	3	119.4	8.3	126.1	9.0	132.6	10.4
150% t_r	1	128.6	8.6	138.7	9.1	148.7	10.0
	2	115.0	7.9	122.7	8.4	130.5	9.5
	3	110.6	7.8	117.4	8.4	124.5	9.4
200% t_r	1	152.0	7.9	169.1	8.2	177.4	8.9
	2	131.6	7.4	143.6	8.0	147.5	8.8
	3	125.1	7.4	137.1	8.1	138.0	8.9

[a] These values were determined at a lateral displacement amplitude slightly less than 25% due to setup capabilities.

It can be observed that as the temperature the specimen is conditioned at is decreased, the effective horizontal stiffness of the specimen increases. This trend is valid at all lateral displacement amplitudes and creates curves that become more parallel to one another as the displacement intervals increase. During the first interval of 25% to 50% t_r, the change in stiffness was approximately 40, 50 and 60 N/mm for each of the 20 °C, 0 °C, -20 °C test specimens. By the 100% to 150% t_r interval, the change in stiffness of each specimen was between 8.1 and 8.8 N/mm. This shows how the change in stiffness converges for all specimens. At 200% t_r full stable rollover occurs and an increase in stiffness is evident in the figure. Each specimen's effective stiffness increases to values greater than values at lower displacement amplitudes, in particular, 100% tr.

The Standard Specification for Plain and Laminated Bearings gives the criteria of a bearing to be accepted for use at low temperatures. It requires that the stiffness at the conditioned temperature be less than four times the room temperature stiffness (AASHTO 2011). This equates to a maximum percent increase of 300% of the room temperature stiffness. Figure 5b shows that the conditioned bearings behaviour is acceptable at all displacement amplitudes tested. The greatest percent increase is only 24% and occurs with the -20 °C specimen at 25% t_r. Accordingly, the FREI were all expected to pass the provided criteria at the current conditioning periods and temperatures.

Another way to analyze the data is on a per cyclic amplitude basis. This is shown in Figure 5c, where the lateral stiffness is plotted versus the conditioning temperature. It is interesting to note that, excluding the previously mentioned discrepancy, the change in stiffness over the three temperatures is approximately constant for each displacement. This indicates that the relationship between stiffness at different temperatures for the same length of

conditioning can potentially be modeled as approximately linear over the +20 °C to -20 °C temperature range. However, more test data is required to confirm this.

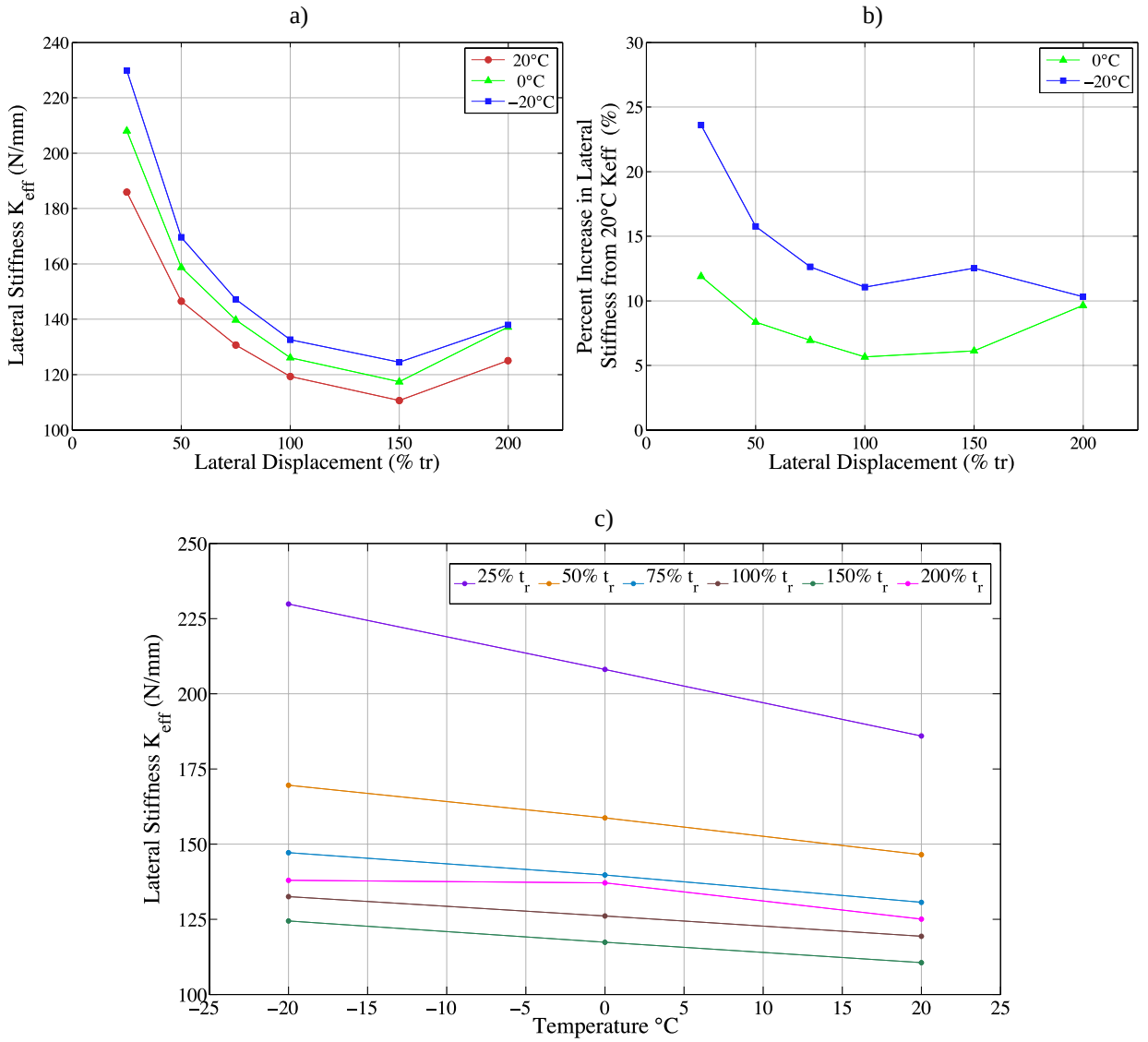

Figure 5: a) Lateral stiffness versus final cycle displacement amplitude.
b) Percent increase in stiffness when compared to 20 °C.
c) Relationship between lateral effective stiffness and temperature at each displacement amplitude.

4.3 Equivalent Viscous Damping Comparison

The damping ratio was determined at all lateral displacements for each specimen and the results are displayed in Figure 6a. The greater level of damping present within the specimens can be explained by the behaviour of the carbon fiber within the FREI. It was found that the addition of fiber reinforcement provides a source of energy dissipation in the bearing, in addition to the inherent properties of natural rubber (Kelly 1999; Toopchi-Nezhad et al. 2007). It has been postulated that in unbonded applications of FREI, as the fibers in the reinforcement bend, the only way to permit this flexure is if the fibers slip past one another. The inherent tension in the fibers, combined with the vertical load on the isolator causes frictional forces to form (Kelly 1999). Energy is dissipated as these forces are overcome and slip between the fibers occurs. It is not expected that the amount of energy dissipated by the fibers increases at lower temperatures.

At lower temperatures the damping ratio increases noticeably. Figure 6b shows this increase in damping at lower temperatures as a percent increase of the damping ratio at 20 °C. For the 25% t_r displacement amplitude, the percent increase in damping ratio is 35% for the -20 °C specimen and 16% for the 0 °C specimen. The percent increase in damping ratio becomes smaller as the amplitude is increased. This trend is only not valid for the 0 °C bearing at 200% t_r and is consistent with the increase in stiffness that was observed at the same temperature and displacement.

A previous study by Kulak and Hughes (1993) on steel reinforced isolators, found that the same trend with respect to temperature occurs. In the study, as the temperature was decreased from 20 °C to -20 °C, the damping ratio increased by approximately 7% at 100% t_r (Kulak and Hughes 1993). The data provided in Figure 6a, shows that an increase of approximately 2% occurred over the same temperature range. The study additionally found that as the displacement amplitude was increased, the damping ratio decreased, which is also consistent with the data presented here (Kulak and Hughes 1993).

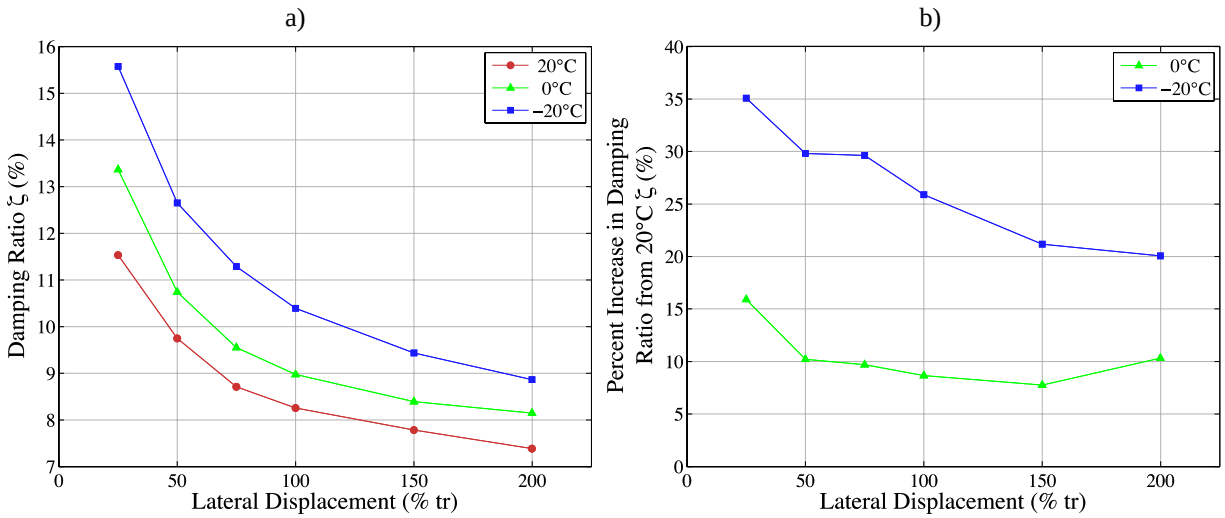

Figure 6: a) Damping ratio versus final cycle displacement amplitude
b) Percent increase in damping ratio when compared to 20 °C

4.4 Mullins Effect and Temperature

It was observed from the hysteresis loops that the stiffness on the final cycle of each lateral displacement was less than that of the first cycle at the same displacement. This occurred for every set of cyclic displacements and can be explained from the properties of the elastomer. Cyclically displacing an elastomer until it reaches the same amplitude as the previous cycle results in the material being loaded, unloaded and then loaded again. During the first cycles, the molecular structure of the elastomer changes as cross-links within it are broken (Marckmann et al. 2002). As a result, subsequent displacements require less force in order to displace the rubber to the same amplitude. This softening of the rubber is called the Mullins effect (Marckmann et al. 2002). As the number of cycles increase, this effect minimizes until the rubber achieves a stable state (Toopchi-Nezhad et al 2008b). The FREI were tested with three fully reversed cycles, as this is the number of cycles stated in both CSA-S6 (2014) and the ASCE Standard for Minimum Design Loads for Buildings and Other Structures (ASCE 2010). The ASCE Standard gives guidance on the amount of softening that is allowed to occur before a room temperature specimen is no longer considered adequate. It states that the effective stiffness at any of the three cycles must be less than or equal to 15 percent of the average effective stiffness of those three cycles (ASCE 2010). It can be seen in Figure 7 that for the room temperature specimen, the percent change between the maximum and minimum effective stiffness values of the three cycles is within 15 percent up to the 150% t_r amplitude. Since the total difference is within the limits, the percent change from the average will also be within the limits. For the 200% t_r cycles, the maximum and minimum effective stiffness cycles must be compared to the average effective stiffness. The values taken from Table 1 have been used to determine that the average stiffness is 136.2 N/mm and the variation from this average is only 11.6 and 8.2 percent for the maximum and minimum effective stiffness cycles, respectively. The room temperature bearing is deemed acceptable based on this criterion. The specimen tested at -20 °C was checked as well in order to determine

if a conditioned bearing can pass the adequacy criteria. At 200% t_r the bearing has a decrease in effective stiffness by approximately 22 percent over the three cycles. Comparing the maximum and minimum stiffness values to the average value, resulted in a 15% increase and 10.6% decrease in stiffness compared to the average value. This is just within the acceptable range and after checking that the bearing at the 150% t_r amplitude is acceptable, the conditioned bearing is deemed adequate as well.

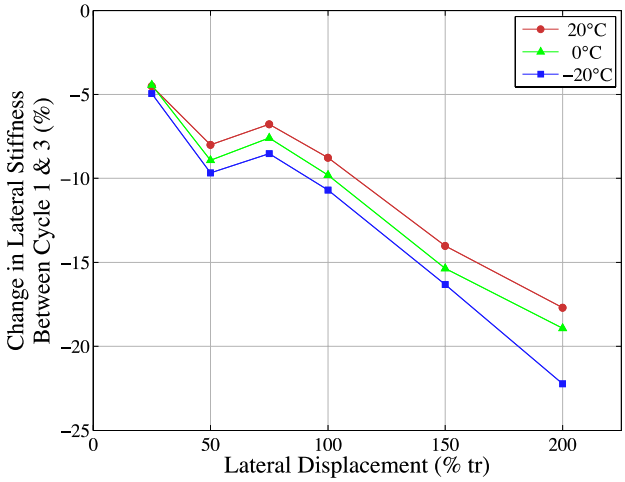

Figure 7: Maximum percent change in effective stiffness between cycles for each lateral displacement amplitude.

5. CONCLUSION

Bearings that are to be used in a bridge application must withstand the same temperatures as the bridge. As a result, it is important to know the behaviour of the bearings at low temperatures. In this study, quarter scale carbon FREI bearings were tested under lateral cyclic deformations at low temperatures, in order to determine their lateral response. For the tests, each specimen was subjected to a single temperature, for a length of 7 days. The three conditioning temperatures were 20 °C, 0 °C and -20 °C. In addition, all specimens were cut to have the same aspect ratio that is known to ensure stable rollover.

The main conclusions to draw from this research are that:

- Hysteresis loops have the same shape at low temperatures as at room temperature.
- Bearings conditioned at lower temperatures have a higher stiffness throughout all lateral displacement amplitudes.
- The maximum increase in stiffness is well within the amount permitted by AASHTO M 251-06 (2011) for low temperature testing.
- Bearings conditioned at lower temperatures, also have a larger damping ratio throughout all lateral displacement amplitudes.
- The Mullins effect on the lateral stiffness is larger for lower temperatures.
- All bearings met clauses outlined in ASCE-7 (2010) limiting the impact of the Mullins effect.

In general, all low temperature bearings performed adequately and can be deemed as providing acceptable lateral performance at low temperatures. The information gathered in this preliminary study will be used to prepare the next phase of the research program. It will involve conditioning lengths that coincide with various standards and a larger range of temperatures that reflect the in-situ temperatures representative of various regions throughout Canada.

ACKNOWLEDGEMENTS

This research was carried out as part of the mandate of the Centre for Effective Design of Structures (CEDS) at McMaster University and is partially funded by the Ontario Ministry of Economic Development and Innovation and by the Natural Sciences and Engineering Research Council of Canada (NSERC).

REFERENCES

Al-Anany Y., Tait M. 2015. A numerical study on the compressive and rotational behavior of fiber reinforced elastomeric isolators (FREI). *Composite Structures*, 133: 1249-1266.

Al-Anany Y., Van Engelen, N. and Tait M. 2016a. An experimental investigation on the vertical and lateral behaviour of unbonded fiber-reinforced elastomeric isolators, *Engineering Structures*, under review.

Al-Anany Y. and Tait M. 2016b. An experimental study of the vertical and rotational behaviour of unbonded fiber-reinforced elastomeric isolators (U-FREI) for bridge applications, *ASCE Journal of Bridge Engineering*, under review.

American Association of State Highway and Transportation Officials (AASHTO). 2011. *M 251-06 Standard Specification for Plain and Laminated Elastomeric Bridge Bearings*, AASHTO, Washington, D.C., USA.

American Society of Civil Engineers. 2010. *Minimum design loads for buildings and other structures*, ASCE/SEI 7-10, New York, USA.

Chopra, A. 2012. *Dynamics of Structures, 4th ed.*, Prentice Hall, Upper Saddle River, NJ, USA.

CAN/CSA-S6-14. 2014. *Canadian Highway Bridge Design Code*, CSA, Mississauga, Ontario, Canada.

Kelly, J. M. 1999. Analysis of Fiber-Reinforced Elastomeric Isolators. *Journal of Seismology and Earthquake Engineering*, 2 (1): 19–34.

Kulak, R.F., Hughes, T.H. 1993. *Frequency and Temperature Dependence of High Damping Elastomers*, Office of Scientific and Technical Information, U.S. Department of Energy, Oak Ridge, Tennessee, USA.

Marckmann, G. et al. 2002. A theory of network alteration for the Mullins effect. *Journal of the Mechanics and Physics of Solids*, 50 (9): 2011–2028.

Murray, R. M. and Detenber, J. D. 1961. First and Second Order Transitions in Neoprene. *Rubber Chemistry and Technology*, 34 (2): 668–685.

Pinarbasi, S., Akyuz, U. and Ozdemir, G. 2007. An Experimental Study On Low Temperature Behavior of Elastomeric Bridge Bearings. *10th World Conference on Seismic Isolation, Energy Dissipation and Active Vibrations Control of Structures*, Anti-Seismic Systems International Society, Istanbul, Turkey.

de Raff, M. G., Tait, J. M., Toopchi-Nezhad, H. 2011. Stability of fiber-reinforced elastomeric bearings in an unbonded application. Journal of Composite Materials, 45 (18); 1873–1884.

Roeder, C. W., Stanton, J. F. and Feller, T. 1989. *Low Temperature Behaviour and Acceptance Criteria for Elastomeric Bridge Bearings*, Transportation Research Board, Washington, D.C., USA.

Roeder, C. W., Stanton, J. F. and Feller, T. 1990. Low-Temperature Performance of Elastomeric Bearings. *Journal of Cold Regions Engineering*, 4 (3): 113-132.

Toopchi-Nezhad, H., Tait, M. J. and Drysdale R. G. 2007. Testing and modelling of square carbon fiber-reinforced elastomeric seismic isolators. *Structural Control and Health Monitoring*, 15: 876–900.

Toopchi-Nezhad, H., Tait, M. J. and Drysdale R. G. 2008a. Lateral Response Evaluation of Fiber-Reinforced Neoprene Seismic Isolators Utilized in an Unbonded Application. *Journal of Structural Engineering*, 134 (10): 1627–1637.

Toopchi-Nezhad, H., Tait, M. J. and Drysdale R. G. 2008b. A Novel Elastomeric Base Isolation System for Seismic Mitigation of Low-Rise Buildings. *14th World Conference on Earthquake Engineering*, Chinese Association of Earthquake Engineering, Beijing, China, Online proceedings.

Van Engelen, N. C., Tait, M. J. and Konstantinidis, D. 2014. Model of the Shear Behavior of Unbonded Fiber-Reinforced Elastomeric Isolators. *Journal of Structural Engineering*, 134 (7).